

Investigation Corrosion and Wear Behavior of Nickel-Nano Silicon Carbide on Stainless Steel 316L

Nawal Mohammed Dawood^{1,a}, Nabaa S. Radhi², Zainab S. Al-Khafaji³

^{1&2}University of Babylon/Department of Metallurgy Engineering/Babylon, Iraq

³Al-Furraat Al-Awsat Distribution Foundation\Ministry of Oil\Babylon, Iraq

³Al-Mustaqbal University College/Department of Engineering/Babylon, Iraq

Mat.newal.mohammed@uobabylon.edu.iq

Keywords: composite coating, electroplated, corrosion, nanoscale and microhardness

Abstract. This study attempts to use a composite coating (co-deposition coating) and assesses, develops the Nickel coatings properties by combining particles of silicon carbide into the electrodeposited solution. The electroplating coating used to coat the stainless-steel samples consisted of Nickel and silicon carbide nanoscale particles having sizes between 70 to 100 nm with various contents equal to 16, 24, 32 and 40 (g/L). The samples were tested by SEM and AFM after electroplating and potentiostatic polarization test in a solution with 3.5% NaCl for investigating the corrosion behaviour. Subsequently, wear resistance and microhardness of these samples were evaluated. A great decrease in the corrosion currents due to the inert nanoparticles' addition was obtained. The corrosion and wear resistances were improved when adding the composite coating.

Introduction

Coating technology is a modern technique that was officially established in the 1950s. Coating or in general called substratum is the surface finishing process of an object [1]. Coatings are applied to the objects for improving the substrate surface properties like lubrication, mechanical properties, wettability, adhesion, wear resistance, corrosion resistance, and scratch resistance. Coating structure has two forms: either a single layer or multiple layers. The single-layer coating consists of only one layer of the material. This layer is mounted on the substrate that was properly prepared using one technological operation or method. The single-layer coating could be formed from either a single-material that constituted of one material (element, compound) or a multi-material [2].

Multi-layer coating is produced from using two or more metals. These layers can be fabricated from one material that separated by means of a sub-layer, or different components where sub-layer is not essential in these cases. The multilayer coating is used to intensify the protection of the substrate [3]. Torabinejad et al. [4] used electrodeposition method to perform tests on Ni-Fe in the presence and without the nano-alumina particles by pulse current and assessed the corrosion and wear resistances. Coating with double-layer of Ni-Cr has been used in the automotive since 1964, which is the simplest electrodeposition multi-layer coating. The fine inert particles electrodeposition on the metal matrix coating steadily increased during since that time. Matrix coatings by Ni and/or Co in the automotive, aircraft, aviation, marine, textile, and nuclear fields. They are also utilized in high pressure valves, parts of engine cylinder, drill fittings, etc. [5].

Composite coating is used to provide a substrate shield that consists of two or more materials in combination. Both reinforcement particles and coating matrix are important parameters that affect the coating properties. Using different techniques, the coating is prepared to satisfy the requirements of various applications. Extra wear and corrosion protections are provided by composite coating. The micro-hardness, corrosion, and wear resistance were improved when using composite coating of Ni-Al₂O₃ [6].

Electrodeposition composite coating incorporates the reduction in the metal ions with undissolved oxide particles (Al₂O₃ [6], TiO₂ [7], SiO₂ [8], MoS₂ [9], ZrO₂ [10]), carbides (SiC [11

and 12], B₄C [13]), and hydroxyapatite [14]. Nickel-silicon carbide structures are one of the most widely used composite coatings in vehicle manufacturing to minimize the engine's corrosion and wear rates. This leads to form and integrated metal/alloy matrix along with micro/nano solid particles. Composite coating properties depend on the integrated particles size, their nature, and their type, which can enhance the essential characteristics of the metal/alloy's substrates. As composite coatings have higher hardness and yield strength compared to pure metals, they mainly used to enhance the wear and corrosion resistances [15]. Several studies attempted to build the model for predicting and describing the particles' co-deposition. Hence, theoretical models have been built to get focus on the mechanism of deposition. Previous literature regarding this matter shows that existence of particle led to un address the rate of metal reaction.

The method of electrodeposition generally applied an electrical current to the metal/alloys for producing a uniform and dense coating having a superior adhesion characteristic to the substrate material. The flexibility and commercial advantages of the electrolysis process have attracted the interest in electrodeposition coating. Electrodeposition coating method is used in parts coating that required exceptional characteristics [16]. Electrodeposition is a major technique for the production of composite coating owing to its advantages, such as homogeneous distribution of particles, high rate of deposition, low cost, operating pressures flexibility and bath temperatures [17]. The applied electrical current to the cathode results in a reduction in the coating material ions owing to the producing the metal/alloy coating. A metallic layer with sufficient electrons is mounted on the substrate material using an aqueous solution [3].

The substrate nature, the plating conditions, the bath purity, and the electrolyte solution structure are all influence the electrodeposit property. To obtain reliable and reproducible results, additional care is necessary for operating and designing the experimental electrodeposition method [18].

In the current work, electrochemical potentiodynamic tests were performed to recognize the effects of coating parameters on the polarization performances of the coated layer. The electrodeposition procedure has been done by using silicon carbide nano powder as an additive to the nickel sulfate solution for the invention of the nickel/silicon carbide nano-composite coatings. The outcomes of electrodeposition parameters such as silicon carbide particles amounts on the coating performance were studied. The codeposition concentration of silicon carbide, microstructures, Vickers microhardness, corrosion, and wear behavior of the coated layer were studied. Pure nickel deposition was formed under the same investigational circumstances for evaluation. The aim was to prepare hard nickel/silicon carbide nano composite coating with good resistance to wear and corrosion behavior.

Experimental Work

Electroplating Process

The base alloy usage in this research was austenitic stainless steel (316L). The nominal constituent of austenitic stainless steel 316L alloy has been explored in Table 1, whereas, Table 2 gives Spectro-chemical constituent of austenitic stainless steel in weight percentages.

Table 1: Preventive Chemical Constituent of Austenitic Stainless Steel 316L in Weight Percentage Rendering to [19]

| EL | Fe | C | Mn | Si | Cr | Ni | P | S | Mo | V | Cu |
|------|------|-------------|-----|-----|-------|-------|---|---|-----|---|----|
| Wt.% | bal. | <0.02-<0.03 | 2.0 | 1.0 | 16-18 | 10-14 | _ | _ | 2-3 | _ | _ |

Table 2: Spectrochemical Constituents of Austenitic Stainless Steel 316L in Weight Percentage

| EL | Fe | C | Mn | Si | Cr | Ni | P | S | Mo | V | Cu |
|------|------|-------|------|------|-------|-------|-------|-------|-------|-------|-------|
| Wt.% | bal. | 0.041 | 1.42 | 0.27 | 19.38 | 10.24 | 0.025 | 0.003 | 0.283 | 0.080 | 0.218 |

Cylindrical moulds were used to prepare the samples for tests. The dimensions of the samples (disc-shaped) are 3 mm for the thickness and 20 mm for the diameter with surface area equal to 5.181 cm^2 . Surface of the samples were prepared as follows:

1. The surfaces of the samples were grinded utilizing grit silicon carbide papers (220, 240, 400, 600, 800, 1000, and 1200). Then, they were cleaned using distilled water for being ready for the electroplating process.
2. Before electrodeposition of Ni-SiC composites, the Ni deposits were obtained in accordance with the following procedures [20]:
 - a. Cold rinsing
 - b. Dipping in 20% HCl (1.098 sp. gr.) at temperature ranged from 21 to 27°C for a minute
 - c. Cold rinsing
 - d. Anodic etching in the wood's nickel-strike bath that contained 240 (g/L) of NiCl_2 and 86 ml/L of HCl with a concentration equal to 37% at temperature of the solution equal to 43°C utilizing a density of deposition current equal to 53.8 mA/cm^2 for 20 seconds
 - e. Plating in the wood's bath at a temperature equal to 43°C using a density of deposition current equal to 0.0538 A/cm^2 for two minutes
 - f. Cold rinsing
3. The electroplating process was conducted utilizing a 1000 ml glass jar with a magnetic stirrer (as shown in Fig. 1) and a power supply that have the ability to provide a voltage and a current up to 20 V and 6 A, respectively.



Fig. 1: Electroplating cell.

Electroplating Baths Composition

The Watts Nickel Plating solution (Watt formulation was invented by Oliver P. Watts in 1916) and the number of nickel-plating alternatives were used for ornamental plating. Even though the ratios of nickel chloride, nickel sulphate, and boric acid may possibly vary depending on the operation, they were collected via the Watts electrolyte. Table 3 lists the typical formulation of the plating solution and its operating parameters.

Table 3: Plating solution components and conditions of deposition, [21].

| Solution | Chemical composition | Conditions of Deposition |
|---------------------|---|---|
| Nickel-SiC Solution | $\text{NiSO}_4 \cdot 6\text{H}_2\text{O} = 240 \text{ g/l}$ $\text{NiCl}_2 \cdot 6\text{H}_2\text{O} = 45 \text{ g/l}$ $\text{H}_3\text{BO}_3 = 25 \text{ g/l}$ $\text{SiC} = 16, 24, 32 \text{ and } 40 \text{ g/l}$ Nano scale, d (70-100) nm | pH = 4.5 Temp = 55°C. Coating time 60 min. Nickel Anodes = (99.9%) Current density = 2.5 (amp/dm ²) |

Heat Treatment Procedure

In order to explain the coating creation process of the nickel-silicon, the prepared samples were subjected to a heat treatment. Vacuumed furnace GSL-1600x was used for the treatment. 10^{-4} torr was the numerical value of the pressure of the furnace for avoiding the problem of oxidation of the base materials throughout the whole procedure.

The procedure of the two-step heat treatment was accomplished for the samples. The samples were heated up from 25 °C to 500 °C within a stable increment of the temperature equal to 10 °C/min. The samples were maintained at 500 °C for 3 hrs. Next, the samples were heated up until 950°C within a stable increment of the temperature (5 °C/min) and maintained 5 hrs at the maximum value of the temperature. After that, furnace cooling process was run for cooling the samples down to temperature of the laboratory. The schematic of the heat treatment is presented in Fig. 2.



Fig. 2: The heat treatment process for coated sample.

Thickness Test

D-5870 HEMER-Sundwing, W. Germany was used for thickness measuring of the layer of Ni-SiC.

Scanning Electron Microscope (SEM)

To measure and identify the grain size, shape, phases, and several characteristics of the boundaries of the grain, SEM is used. All of these characteristics are dissimilar. A magnification of 2.00kx was used for the microstructure evaluation.

Atomic Force Microscope

To test the film morphology (depth and roughness), AFM (Atomic Force Microscopy) of the contact mode known as spm AA3000 Angstrom advanced Inc., USA was utilized.

Hardness Test

TH-717 Digital Micro Vickers Hardness Tester based on Vickers hardness model was used for measuring the Ni-SiC layer hardness at a load of 200N for 20 seconds as holding time.

Potentiostatic Polarization Test

The test of the Potentiostatic Polarization was accomplished based on ASTM G5-94(2011) e1. Mlab Sci-Electrochemica was the test type that used for that within the salt solution for the coated and uncoated samples at 30°C. The experiments of the Potentiostatic polarization were done in 3 cells of electrode. These cells contain solution of electrolytes salt. The rate of corrosion can be calculated by using Eq. 1 as:

$$\text{Rate of corrosion (mpy)} = 0.1288 \text{ icorr (E.W.)} / \dot{A} \cdot \rho \quad (1)$$

where E.W is the equivalent weight (g/eq.), \dot{A} is the area measured by (cm^2), ρ is the density measured by (g/cm^3), icorr is the density of the current measured by ($\mu\text{A/cm}^2$), and the number 0.1288 is the factor of conversion for metric and time.

The percentage of improvement for the coated samples can be calculated [22]:

$$\text{Improvement percentage} = (\text{CR}^0 - \text{CR}) / \text{CR}^0 * 100 \quad (2)$$

Where:

CR° =the rate of corrosion for master specimen (without coating).

CR =the rate of corrosion for coated specimen (with Ni or (Ni-SiC)).

Wear Resistance Test

Based on ASTM (G99-04), samples of 3 mm thickness and 20 mm diameter were fabricated by Ni-SiC process. A sensitive electrical balance model (M254A) was used to measure the weight of the samples within +0.0001 accuracy. The idea of the pin on disk was utilized to measure the dry wear. Type of wear tester defined as (MT-4003, 10.0 version) was used. The tested samples were placed against a conventional spinning steel disk with 850 HV hardness as a pin. Four values of the normal forces on the pin are selected (10, 20, 30 and 40) N, the diameter of the pin is 10 mm, while the diameter of the used disk is 30 mm. The radius of wear track (R) is 5mm. The rotational speed of the disk (ω) is 300 rpm. The sample then weighted after 5, 10, 15, and 20 minutes in order to calculate the loss of weight. The weight loss or reduction was converted to the loss of volume by using Eqn. 3 as [23]:

$$\text{Loss in volume (mm}^3\text{)} = \text{loss in mass (g)} / \text{density (g/mm}^3\text{)} \quad (3)$$

where the loss of weight is the difference between the sample weights before and after the test.

The Results of Experimental Work and Discussion

Thickness Results

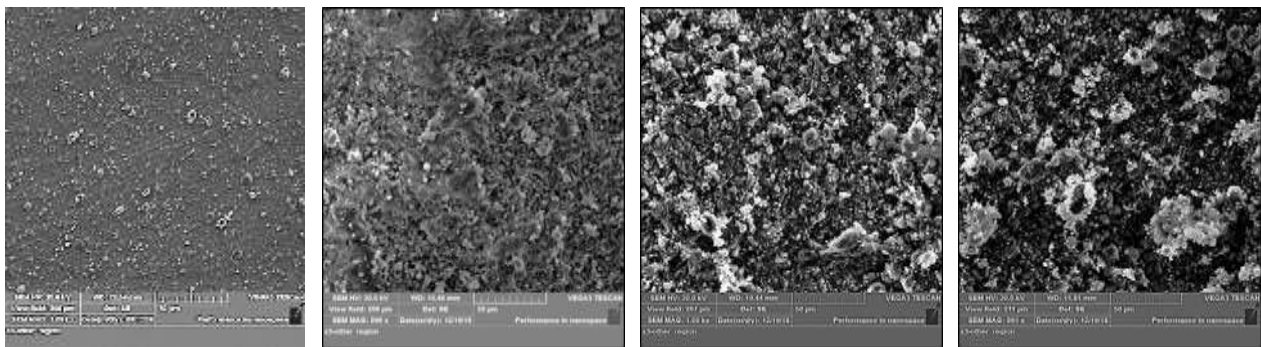
For coating samples, the thicknesses of Ni-SiC were 40.7, 42.3, 44.5 and 47.9 (μm) within 16, 24, 32, and 40 (g/L), respectively. The results showed that the deposit rates of the last layers of coating were great due to the high level of diffusivity of the species produced by SiC presence. Though, thickness rate increase as the particles amount of SiC increase as can be noticed in Table 4.

Table 4: The Thickness of Ni-SiC Layer's Coating

| Samples Conditions | Coating Thickness(μm) |
|------------------------------|------------------------------------|
| Nickel-Silicon carbide,16g/l | 40.7 |
| Nickel-Silicon carbide,24g/l | 42.3 |
| Nickel-Silicon carbide,32g/l | 44.5 |
| Nickel-Silicon carbide,40g/l | 47.9 |

Scanning Electron Microscope (SEM)

Fig. 3 established SEM microstructure of Ni-SiC electrodeposited samples for various amounts of SiC (i.e. 16, 24, 32 and 40 g/L). As noted from this figure the SiC amount had increased. The SiC particles were placed to obtain clusters which appear as a heavy and agglomerated composition over the base material.



(a): Ni-SiC 16g/l,

(b): Ni-SiC24g/l,

(c): Ni-SiC 32g/l

(d): Ni-SiC 40g/l

Fig. 3: Coating layers SEM micrograph morphology with different Ni-SiC concentrations: (a) 16 (g/L), (b) 24 (g/L), (c) 32(g/L), and (d) 40 (g/L)

Atomic Force Microscope (AFM)

Fig .4 shows the results from the atomic force microscopy of the composite coating surface. Here, it notes that the surface was smoother when the SiC concentration of 16 (g/L) was used and after that, the surface roughness continued to increase with an increase in the concentration of silicon carbide in the coating solution until it reached the roughest surface when the SiC concentration was 40 (g/L).

Hardness Test Results

Hardness test was accomplished to find out the coating of Ni-SiC electrodeposited influence on the values of hardness 260 HV of stainless steel. It was also accomplished to find the influence of SiC addition at 70-100 nm as the size of particle for various amounts of nickel solution equal to 16, 24, 32 and 40 (g/L) on the values of the hardness of stainless steel and Ni coating. Table 5 presents the hardness test results for samples of the stainless steel and the layers of Ni-SiC for 16, 24, 32 and 40 (g/L) of SiC. The variation in the hardness detected between Ni-SiC is owing to the variance in the fractional volume of SiC for both layers. Material's hardness was obviously influenced by the particles size and is mathematically clarified by the relationship of Hall-Petch, which states, [12]:

$$HV = H_o + K/\sqrt{d} \quad (4)$$

Whereas:

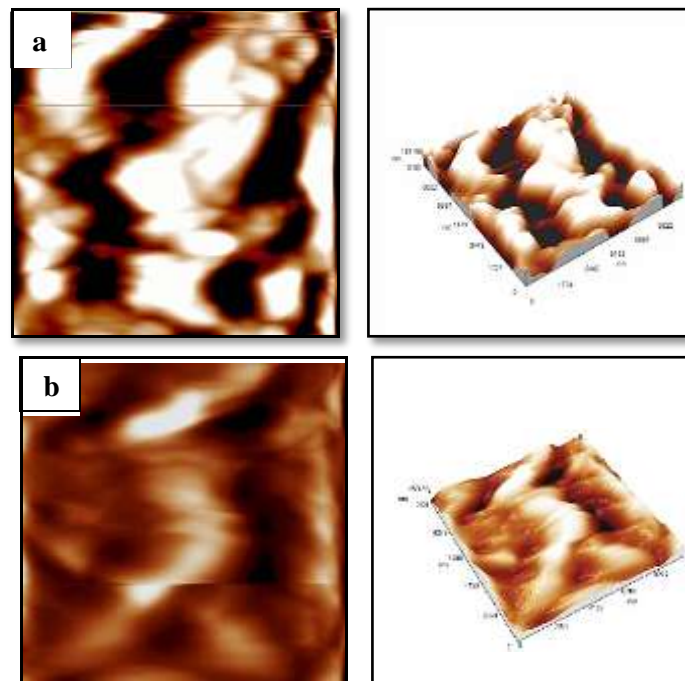
HV: Hardness of material with small grain size.

Ho: Hardness material is multi-size grain (polycrystalline grain size).

K: Constant, represents the slope of the HV hardness when drawing against $(d)^{1/2}$ and is based on the material kind.

d: Diameter of the particle.

The Hall-Petch relationship is one theory that explains why ultra-fine microstructures have higher hardness values 520 HV when compared to the coarser-grained ones with the same hardened material.



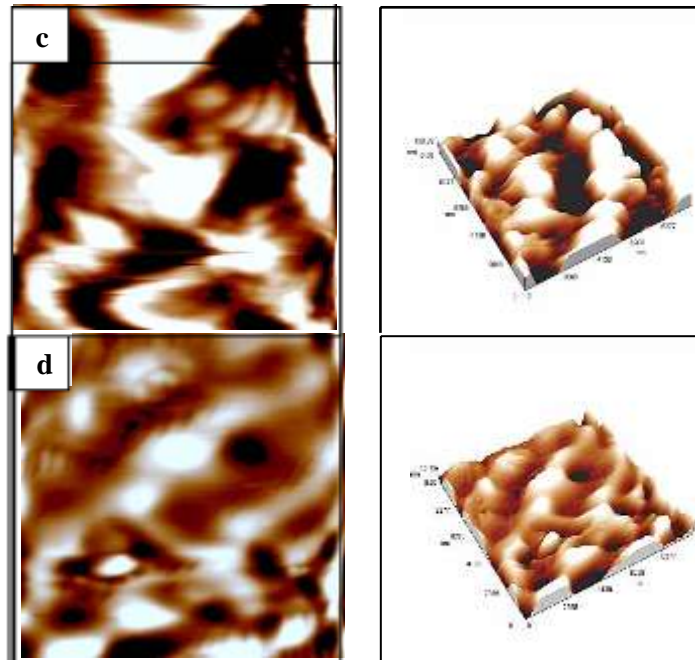


Fig. 4: AFM Pattern of specimen at (a): Ni-SiC 16g/l, (b): Ni- SiC 24g/l, (c): Ni-SiC 32g/l (d): Ni-SiC 40g/l

Table 5: The hardness values of coated layers

| Samples Conditions | Vickers hardness (HV) |
|------------------------------|-----------------------|
| Uncoated | 260 |
| Nickel-Silicon carbide,16g/l | 310 |
| Nickel-Silicon carbide,24g/l | 390 |
| Nickel-Silicon carbide,32g/l | 470 |
| Nickel-Silicon carbide,40g/l | 520 |

Corrosion Tests

Potentiostatic Polarization Tests

Figure 5 shows the polarisation diagrams of all samples and the E_{corr} . (mV), I_{corr} . (μ A). The rate of corrosion has been established in Table 6. Results of this Table show a stable behaviour of SiC coating layer. The resistance of the corrosion has been enhanced. In addition, the SiC coating is capable to make some of important features as compared to the materials where the characteristics of bulk materials are not affected [24, 25]. In addition, SiC presence in the coating layer can increase the resistance of corrosion of the coated samples [24, 26].

With addition of nano-size of SiC particles, the porosity decreased. The main reason for that, the nano-size considerably decreases both of current density of corrosion and the porosity because of pores filling by the nano-size particles. The nano-size particles decreased the current density when incorporation into Nickel solution as shown by Table 6.

Wear Tests

The losses of the weight were actually converted to losses in the volume using each density of sample. Figure 6 shows the wear test results under action of similar conditions mentioned previously (load: 10N - 40N, step of 10N), respectively, and 300 rpm, and (time: 5 – 20, step of 5 minutes)

It is noted that the optimum thickness is (47.9 μ m). However, cracks in spall are developed with further increasing in the thickness above the optimum one. In addition, layer thickness beyond 40 μ m is not working as a protective layer. Fig. 6 holds the growth the results in greater rate of wear

at the steady state due to increase the deformation of the strain rate of the sub-surface. Regarding this results, similar conclusions were presented by Srivastava et al. [27] for the range of sliding. The rate of wear showed to linearly increasing for the greater distance of the sliding. The coating of electroplated nickel is enhanced and showed better characteristics as compared to the coating of standard coarse- crystalline. The changes in the characteristics are enhanced in the micro-hardness or strength, adhesion increase, wear increase, corrosion resistance.

Increasing of the load led to increase the friction between the surfaces of the rotating disc and the sample. In addition, loss of the volume was increased with time due to enhancement in the loss of particles because of the frictional force. Further, the results showed that the loss of volume decreased dramatically as silicon carbide amount increase. The lower value of the volume loss was noticed for the composite contains the highest silicon carbide amount (32 SiC g/L). This might extend the particles of SiC function in coated layers by increasing both wear resistance and hardness. Spalling can be attributed to the thick layer because of defects and adhesive inner loss that noticed after 15 min from loading in the covered layer of 40 SiC (g/L) [28].

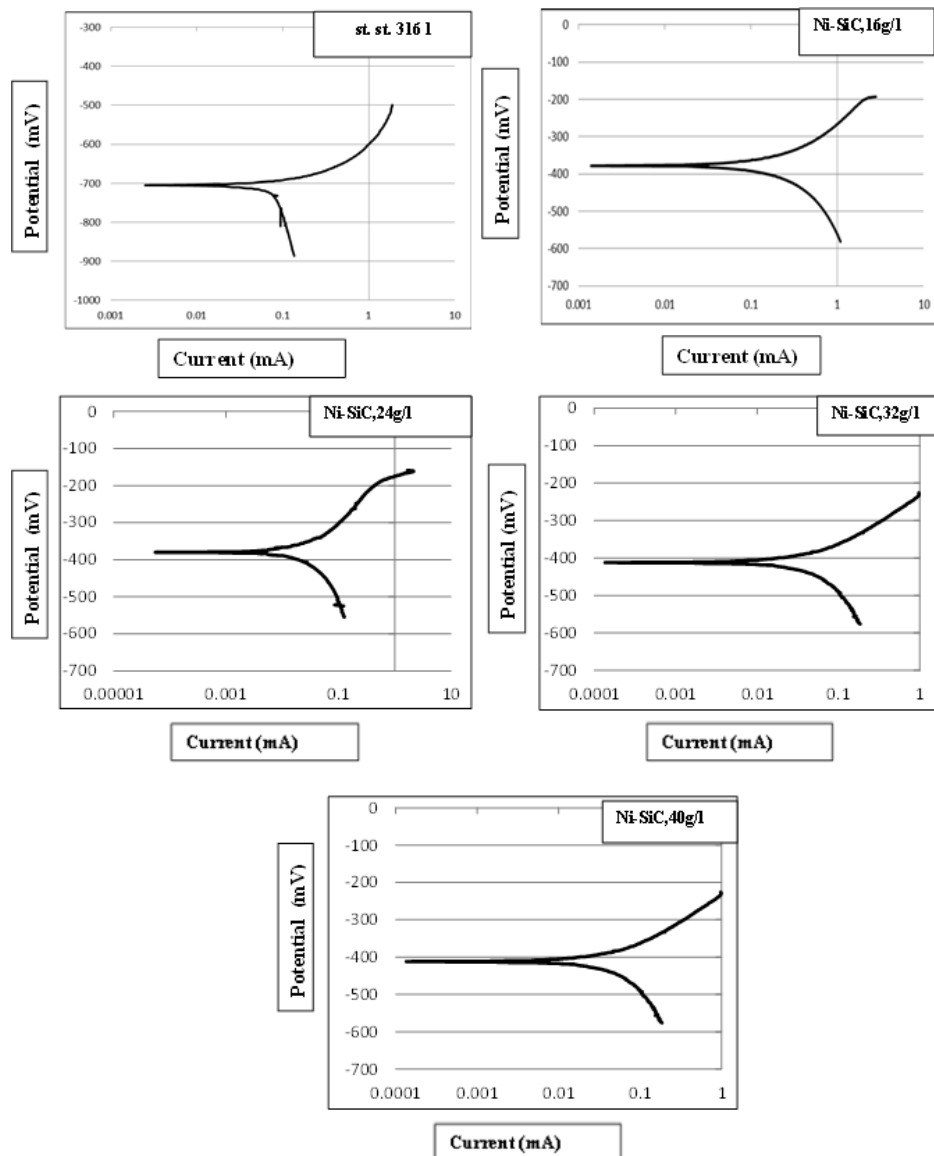


Figure5: The polarisation curves of st.st.316L without and with (Ni-SiC) coated samples at 30 °C

Table 6: The potential of corrosion (E_{corr}), corrosion current (I_{corr}), and percentage of improvement of coated samples in a salt solution at 30°C

| Substrate | E_{corr} . (mV) | I_{corr} . (μ A) | Corrosion rate (mpy) |
|-------------------------------|-------------------|-------------------------|----------------------|
| st. st. 316 L(uncoated) | -707.1 | 54.94 | 0.9284 |
| Nickel-Silicon carbide,16 g/l | -377.8 | 29.19 | 0.4933 |
| Nickel-Silicon carbide,24 g/l | -380 | 6.31 | 0.1066 |
| Nickel-Silicon carbide,32 g/l | -411.1 | 5.91 | 0.0998 |
| Nickel-Silicon carbide,40 g/l | -50 | 5.05 | 0.0853 |

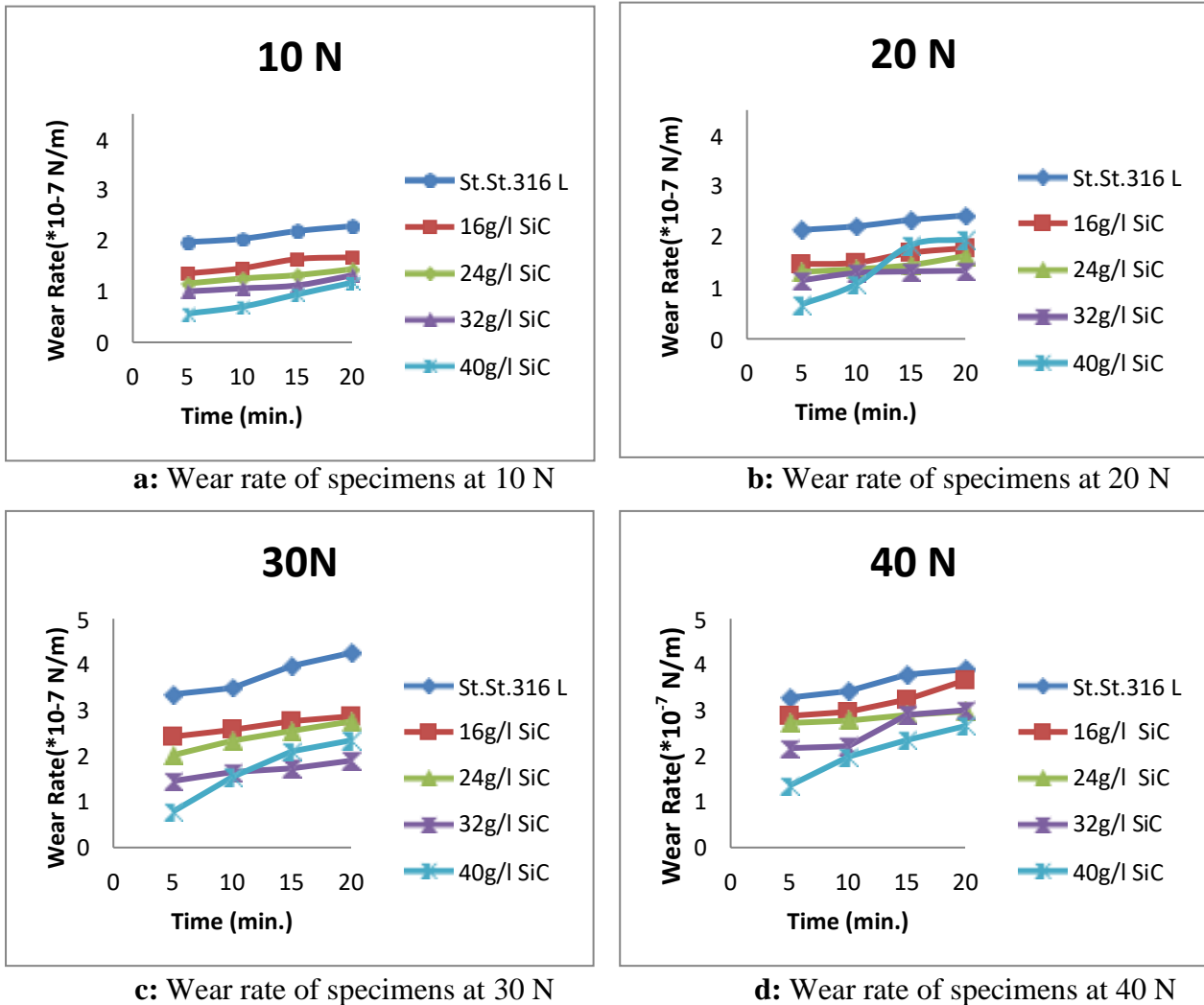


Fig. 6: Wear rate of samples (10, 20, 30, and 40N)

Conclusions

1. For all coatings (composite coating Ni-SiC), the coated substrates were completely enclosed by a layer of composite of nano particles of 70-100 nm in average size of grain.
2. The Ni-SiC composite layer demonstrates a stable structure with higher mechanical bonding and an exceptional crystallization for the surface because of the good combination of nickel matrix and SiC.
3. The Ni-SiC composite layer highly decreased the stainless steel 316L corrosion rate in 3.5% NaCl solution, while maximum enhancement is 90.81% and minimum rate of corrosion is 0.08531mpy when the SiC concentration is 40 (g/L) in coated solution.

4. The stainless steel 316L sample has the highest wear rate at 40 (N) and the rate of wear decreased by 34% when the samples were coated by 32 (g/L) of Ni-SiC.
5. Vickers hardness increased by 19%, 50%, 81%, and 100% for Ni-SiC equal to 16, 24, 32, and 40 (g/L) respectively.

References

- [1] K. C. Ludema, Friction, Wear, Lubrication: A Textbook in Tribology, CRC Press, Boca Raton, FL, 1998.
- [2] W. Q. Liu, W.N. Lei, C.Y. Wang, H.F. Qian, L.H. Ding, Ni-SiC nanocomposites electroplating process under ultrasonic and agitation, *Integr. Ferroelectr.*, 167, 192–198, 2016.
- [3] T. Wierzchon, T. Burakowski, Surface Engineering of Metals Principles, Equipment, Technologies, CRC Press LLC, New York, Washington, DC, 1999.
- [4] V. Torabinejad, A. S. Rouhaghdam, M. Aliofkhazraei, M. H. Allahyarzadeh, Electrodeposition of Ni-Fe and Ni-Fe- (Nano Al₂O₃) multilayer coatings, *J. Alloy. Compd.*, 657, 526–536, 2016. DOI: 10.1016/j.jallcom.2015.10.154.
- [5] L. Benea, E. Danaila, J. Celis, Influence of electro-co-deposition parameters on nano-TiO₂ inclusion into nickel matrix and properties characterization of nanocomposite coatings obtained, *Mater. Sci. Eng. A.*, 610, 106–115, 2014. DOI: 10.1016/j.msea.2014.05.028.
- [6] S. A. Asi, M. Mondal, S. Dayal, S. Kumar, Electro deposition of nickel-alumina composite coating, *Mater. Today Proc.*, 3042–3048, 2015. DOI: 10.1016/j.matpr.2015.07.292.
- [7] R. P. Socha, P. Nowak, K. Laajalehto, J. Vayrynen, Particle electrode surface interaction during nickel electrodeposition from suspensions containing SiC and SiO₂ particles. *Colloids Surf. A Physicochem. Eng. Asp.*, 235, 45–55, 2004. DOI: 10.1016/j.colsurfa.2004.01.011.
- [8] S. A. Lajevardi, T. Shahrabi, Effects of pulse electrodeposition parameters on the properties of Ni-TiO₂ nanocomposite coatings, *Appl. Surf. Sci.*, 256, 6775–6781, 2010. DOI: 10.1016/j.apsusc.2010.04.088.
- [9] W. Wang, F. Y. Hou, H. Wang, H. T. Guo, fabrication and characterization of Ni-ZrO₂ composite nano-coatings by pulse electrodeposition, *Scripta Materialia*, 53, 613–618, 2005. DOI: 10.1016/j.scriptamat.2005.04.002.
- [10] M. F. Cardinal, P. A. Castro, J. Baxi, H. Liang, F. J. Williams, characterization and frictional behavior of nanostructured Ni-W-MoS₂ composite coatings, *Surf. Coat. Technol.*, 204, 85–90, 2009. DOI: 10.1016/j.surfcoat.2009.06.037.
- [11] A. K. Rajah, J. K. Ahmad, N. S. Radhi, Investigation some properties of (Zn-Ni-SiC) composites coating on low carbon steel, *The Iraqi Journal for Mechanical – and Materials Engineering*, 2018.
- [12] J. K. Ahmad, N. S. Radhi, Improvement the hardness and wear of (Zn-Ni) coating layer by adding silicon carbide, *The Iraqi Journal For Mechanical And Material Engineering*, 11 (3), 2011.
- [13] N. K. Shrestha, M. Kawai, T. Sajin, Co-deposition of B₄C particles and nickel under the influence of a redox-active surfactant and anti-wear property of the coatings, *Surf. Coat. Technol.*, 2414–2419, 2005. DOI: 10.1016/j.surfcoat.2004.08.192.
- [14] A. W. Rajih, N. M. Dawood, F. S. Rasheed, Corrosion protection of 316L stainless steel by HA coating via pulsed laser deposition technique, *J. of Eng. and App. Sci.*, 13 (24) 10221–10231, 2018.

-
- [15] S. Ozkan, G. Hapc, G. Orhan, Electrodeposited Ni/SiC nanocomposite coatings and evaluation of wear and corrosion properties, *Surf. Coat. Technol.*, 232, 734–741, 2013. DOI: 10.1016/j.surfcoat.2013.06.089.
- [16] J. R. Roos, J. P. Celis, H. Kelchtermans, K. U. Leuven, Dispersion-hardened electrolytic copper-alumina coatings, *Thin Solid Films*, 54, 173–182, 1978. DOI: 10.1016/0040-6090(78)90196-7.
- [17] B. P. Aghery, M. Farzam, A. B. Mousavi, M. Hosseini, Ni–TiO₂ nanocomposite coating with high resistance to corrosion and wear, *Surf. Coat. Technol.*, 204, 3804–3810, 2010. DOI: 10.1016/j.surfcoat.2010.04.061.
- [18] C. R. Raghavendra, S. Basavarajappa, I. Sogalad, Electrodeposition of Ni-Al₂O₃ nano composite coating and evaluation of wear characteristics, *IOP Conf. Series: Mater. Sci. Eng.*, 2016. DOI: 10.1088/1757-899X/149/1/012110.
- [19] D. Talbot and L. Talbot, *Corrosion Science and Technology*, CRC Press LLC, 1998.
- [20] A. K. Graham, *Electroplating Engineering Handbook*, p.198. Carnes Publication Service. Inc. USA, 1971.
- [21] C. A. Loto, Electroless nickel plating—A review, *Silicon*, 8 (2) 177–186, 2016.
- [22] K. W. NG, H. C. Man and T.M. Yue, Characterization and corrosion study of Ni Ti laser surface alloyed with Nb or Co, 257 (8) 32 G9, 2011.
- [23] K. N. Kadhim, H. Ahmed, The effects of uniform transverse magnetic field on local flow and velocity profile, *International Journal of Civil Engineering and Technology (IJCIET)*, 7 (2) March-April, 140–151, 2016.
- [24] S. Ajay, R. Abhinandan, Study of Hydroxyapatite and Hydroxyapatite-Chitosan Composite Coatings on Stainless Steel by Electrophoretic Deposition Method, National Institute of Technology, 2010.
- [25] M. M. Shalabi, J. G. Wolke, V. M. Jansen, Evaluation of bone response to titanium – coated Polymethacrylate Resin (PMMA) implants by X-ray tomography, *J. Mater sic. Mater Med.*, 18, 2033–2039, 2007.
- [26] J. A. Roether, S. Deb, The effect of surface treatment of hydroxyapatite on the properties of bioactive bone cement, *J. of Mater. Sci., Material in Medicine*, 15, 413–418, 2004.
- [27] M. Srivastava, V. K.W. Grips, K.S. Rajma, Influence of SiC, Si₃N₄ and Al₂O₃ particles on the structure and properties of electrodeposited Ni, *Mater. Lett.*, 62, 3487–3489, 2008. DOI: 10.1016/j.matlet.2008.03.008.
- [28] A. H. Haleem, N. M. Dawood, Investigation the effects of zirconium addition on wear and corrosion behavior of Alpha-Brass Alloy (Cu-Zn30), *Int. J. Mech. Eng. Technol. (IJMET)*, 9 (12, December) 844–857, 2018.
- [29] N. M. Dawood, T. A. Jasim, F. S. Zaid, Corrosion behavior of electro- deposited nickel aluminium composite coating on the stainless steel 316L, *Int. J. Eng. Technol.*, 7 (4) 5501–5505, 2018.